Journal of Bio- and Tribo-Corrosion (2020) 6:76
https://doi.org/10.1007/s40735-020-00368-5

Experimental and Theoretical Evaluation of *Acacia catechu* Extract as a Natural, Economical and Effective Corrosion Inhibitor for Mild Steel in an Acidic Environment

Rajesh Haldhar[1] · Dwarika Prasad[1] · Nishant Bhardwaj[1]

Received: 9 January 2019 / Revised: 23 April 2020 / Accepted: 7 May 2020 / Published online: 21 May 2020

Abstract
The corrosion inhibition of the *Acacia catechu* bark was tested on mild steel in a 0.5 M sulphuric acid solution using weight loss, Tafel and EIS. *A. catechu* showed its best corrosion resistance of 93.85% at a concentration of 600 mg/L. SEM and AFM were used to verify the formation of a protective layer on the surface of the mild steel. The adsorption phenomenon was verified using UV–Vis. spectroscopic technique while FT-IR confirmed the presence of different functional groups containing heteroatoms. The adsorption of the inhibitory molecules on the surface of the mild steel followed the Langmuir adsorption isotherm. Theoretical studies were carried out as a supplementary study. All the results obtained to assure that the bark extracts of *A. catechu* can create an effective blocking layer and control the corrosion process.

Keywords Mild steel · Natural corrosion inhibitor · EIS · Polarization · Weight loss · SEM · theoretical studies

1 Introduction

Mild steel is the alloy which is easily available with its outstanding mechanical properties in construction, industrial process and fabrication [1]. The main problem of using mild steel is their tendency to corrosion in contact with the aggressive medium such as sulphuric acid solution [2, 3]. As it is well known that acid solutions are widely used in the various industrial process for pickling, descaling and cleaning. The organic molecules used as inhibitors are adsorbed on the surface of the metal through their π-electrons system and heteroatoms such as S, P, N, O [4–7]. This adsorption is either chemical (chemisorption) or physical (physisorption). The organic inhibitors, which exist in plant extract, are eco-friendly, economical and effective [8, 9]. As we know most of the natural products are biodegradable and non-toxic. It has easy availability in the market. Several studies have been reported by the various researcher using such natural products as corrosion inhibitor for different metals in different media [10–19]. But most of the green corrosion inhibitor took higher inhibitor concentration to show their highest inhibition performance.

Acacia catechu is a 9–12 m tall tree. This herb is deciduous and has short snared spines. It belongs to the *Leguminosae* family and known as Cutch tree, Black catechu, and Terra japonica. These are usually found all around India, eastern slopes of the Western Ghats. The bark of *A. catechu* is very effectively accessible in the business sector. *A. catechu* holds phenolic compounds (3R, 4R)-3-(3,4-dihydroxyphenyl)-4-hydroxcyclohexane **[1]** and (4R)-5-(1-(3,4-dihydrophenyl)-3-oxybutyl)-dihydrofuran-2(3H)-one **[2]** [20, 21]. Figure 1 shows the image of *A. catechu* barks and its principal phytochemical constituents.

The current observation is expected for the extraction of *A. catechu* bark and analyse the corrosion inhibition properties in the corrosive medium which depends upon electrochemical examinations and weight reduction estimations. Likewise, adsorption of inhibitor molecules on the mild steel surface has been contemplated utilizing AFM and SEM. FT-IR and UV–vis. spectroscopic procedures have been done to check the presence of functional groups and the adsorption phenomenon. All the test results were associated with the hypothetical (theoretical) information to the better comprehend the adsorption phenomenon.

✉ Dwarika Prasad
dwarika123.maithani@gmail.com

[1] Department of Chemistry, Shri Guru Ram Rai University, Dehradun 248001, India

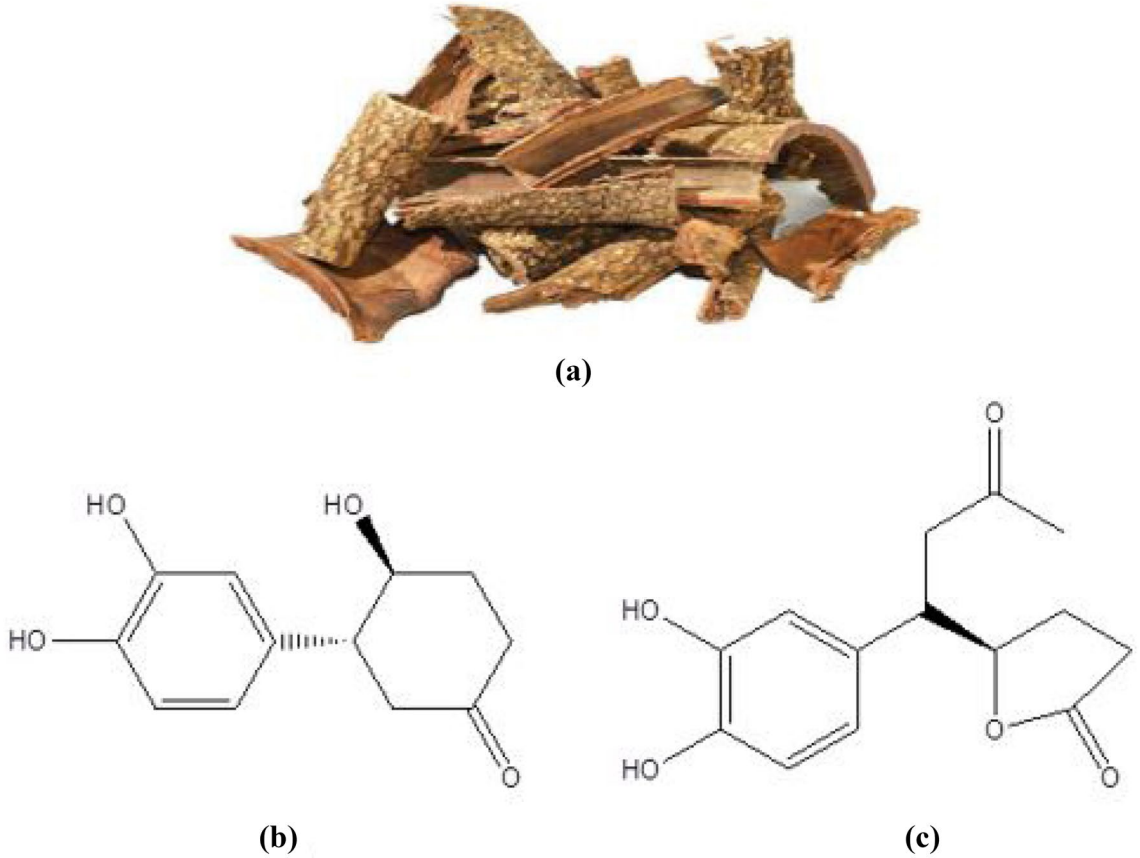

Fig. 1 **a** *Acacia catechu* barks image and their main chemical components, **b** Compound **[1]** and **c** Compound **[2]**

2 Experimental Techniques

2.1 Methodology for Inhibitor, Applicable Electrode and Electrolytes Preparation

Fresh *A. catechu* bark was collected and validated by Dr. Arbeen Ahmad Bhat in the Department of Biotechnology, LPU, Punjab (INDIA). The crude material was thoroughly washed under running water followed by sterile distilled water and dried in the shade. They were grinded to convert in powder. The sample was approximately 100 g of the powder was extracted in a 500 mL round bottom flask with 250 mL of water as the solvent. The filtrate was collected and concentrated using a rotary evaporator under controlled temperature and pressure conditions. The extracts were concentrated to dryness to give a crude residue. Followed by this procedure, around 20% of extract yield with the pH value of around 8 was obtained. 1 cm × 1 cm × 0.03 cm-shaped mild steel specimens were used in weight loss estimations and electrochemical analysis. The chemical composition of the used mild steel specimen is listed in Table 1. The mild steel specimens were abraded with emery paper of grade 100, 300, 600, 800, 1000 and 1200 then washed with distilled water and acetone, dried again and finally kept in a desiccator until used. The sulphuric acid was diluted to 0.5 M H_2SO_4 to use as the corrosive medium. The test solution with specific concentrations (100–600 mg/L) was obtained by diluting plant extract with 0.5 M sulphuric acid solution.

2.2 Weight Loss Estimations

Weight loss estimates were made according to the ASTM method G 31-72 for 24 h [22]. All estimates of weight loss were made at 298 K using a water-circulated thermostat.

Table 1 Elemental composition of used mild steel

Element symbol	Fe	Ni	P	Mn	Cr	Cu	C	Si
% Composition	97.83	0.27	0.12	0.43	0.45	0.43	0.08	0.39

Confidence values were obtained by repeating the experiments three times.

2.3 Electrochemical Studies

Electrochemical impedance spectroscopy (EIS) and potentiodynamic polarization measurements (Tafel) were performed using the CHI760C electrochemical workstation. Experiments were performed at 298 K in 0.5 M sulphuric acid, including various concentrations (100–600 mg/L) of inhibitor. A traditional three-electrode system was used where mild steel with a working area of 1 cm^2 was used as working electrode. The platinum electrode used as an auxiliary electrode and the saturated calomel electrode (SCE) coupled to a luggin capillary was used as the reference electrode. Before each experiment, the working electrode was immersed in the test solution for 60 min to stabilized corrosion potential values (E_{corr}). The polarization curves were recorded at ± 250 mV versus SCE with a scanning speed of 1 mV/s. The EIS spectra were scanned with a frequency range of 100 kHz to 0.01 Hz with a signal amplitude perturbation of 0.005 V.

2.4 Surface Investigations

For the surface analysis, scanning electron microscope (SEM-Model: LEO-435 VP) and atomic force microscope (AFM-Model: NT-MDT-INTEGRA) images of pre-treated mild steel specimen in 0.5 M sulphuric acid, without and with the inhibitor extract (600 mg/L) for 24 h at 298 K, were taken out.

2.5 UV–Visible and FT-IR Spectroscopic Analysis

The UV–Visible spectra of the inhibitor solution before and after immersion of mild steel sample for 24 h at 298 K were taken using Shimadzu UV-1800 UV–Visible absorption spectrophotometer. Then, they were used to explain the mechanism of inhibition. For verification of the main functional groups present in the inhibitor extract, the FT-IR spectrum was taken. The vegetal extract mixed with the KBr pellet for FT-IR analysis in the Shimadzu FT-IR 8400S spectrophotometer with wave number 400–4000 cm^{-1}.

2.6 Theoretical Studies

Theoretical studies were carried out to a deeper understanding of the adsorption mechanism. Quantum chemical calculations were used as theoretical studies. It is a well-known fact that the extract of plants has several phytochemical constituents. For the theoretical studies, we followed the presence of two main phytochemical constituents in the plant extract *A. catechu*. Quantum chemical calculations were conducted using density functional theory (DFT) with Hyperchem 8.0 software. Key parameters were obtained from the optimized structures [23].

3 Results and Discussion

3.1 FT-IR and UV–Vis. Spectroscopic Techniques

FT-IR spectroscopic technique carried out for identification of various functional groups, containing different heteroatoms. Figure 2 shows the FT-IR spectra of pure inhibitor. In pure inhibitor, a peak at 3379.40 cm^{-1} is due to the OH starching. A peak at 2926.11 cm^{-1} in pure inhibitor is due to C–H starching of π-system. A peak at 1631.83 cm^{-1} in pure inhibitor is due to C=O bending. A peak at 1041.60 cm^{-1} in pure inhibitor is due to C–O starching. The presence of these peaks verified the presence of described functional groups containing heteroatoms (O) along with the π-system [24].

To verify the adsorption phenomenon, UV–visible spectroscopy technique has been used. UV–vis. analysis

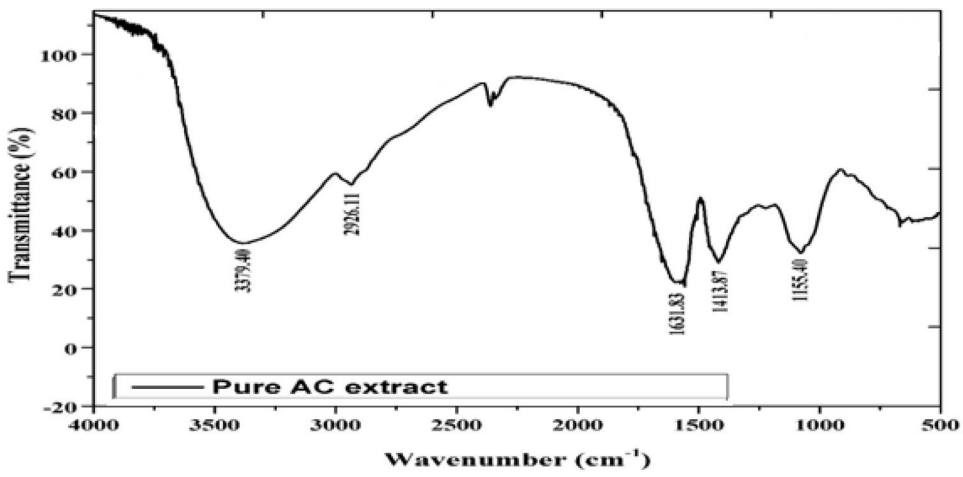

Fig. 2 FT-IR spectra of pure *A. catechu* bark extract

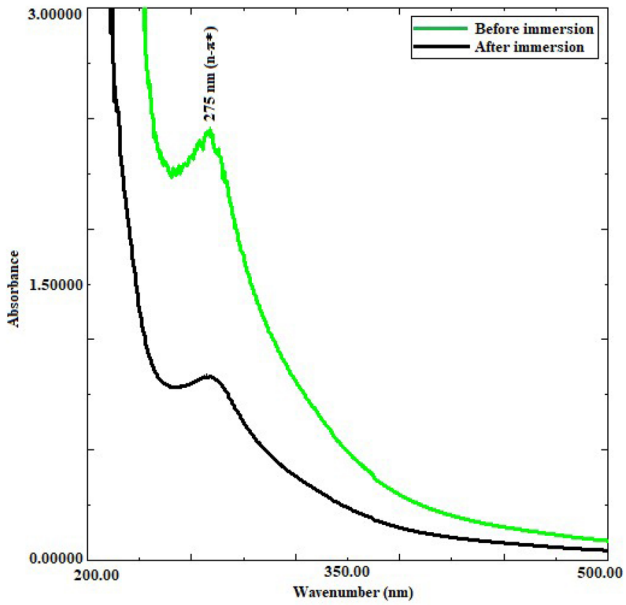

Fig. 3 UV–vis. spectra of *A. catechu* extract after and before the corrosion test

has been done in two modes, before and after the corrosion test. Figure 3 shows the UV–vis. spectra of inhibitor. In this figure, two spectra have been shown one for UV–vis. spectra before the corrosion test and the second one is after the corrosion test. Before the corrosion test inhibitor shows an adsorption peak at 275 nm. This peak can be assigned as n-π* transition. With the help of Fig. 3, we conclude that the graph shows low adsorption peaks after the corrosion test. In the comparison between both the spectra, a significant change has been found in the adsorption band because of the inhibitor molecules get adsorbed on the mild steel surface [25].

3.2 Weight loss estimations and adsorption studies

The weight loss method is the simplest technique for obtaining a basic idea of the relationship between inhibition efficiency and inhibitor concentration. The corrosion rate was calculated using the following equation:

$$C_R = \frac{K \times W}{A \times t \times \rho} \tag{1}$$

whereC_R represents the corrosion rate (mmy^{-1}) of the inhibiting molecules, W represents the weight loss of mild steel (g), K is constant equal to 8.76×10^4, and ρ density of Fe (g cm^{-3}), which is 7.86 (g cm^{-3}). The effectiveness of the inhibition and coverage values of the surface was calculated by the following equations:

$$\mathrm{IE}(\%) = \frac{C_R^0 - C_R^i}{C_R^0} \times 100 \tag{2}$$

$$\theta = \frac{C_R^0 - C_R^i}{C_R^0} \tag{3}$$

where θ is the value of the surface coverage, and C_R^i and C_R^0 is the corrosion rate of the mild steel sample in the presence and absence of the inhibitor, respectively.

The results obtained from the weight loss estimates are listed in Table 2, which shows an increase in inhibitor concentration, decrease in the rate of corrosion, and increase in the inhibition performance. The highest inhibition efficiency of 91.13% was achieved at 600 mg/L inhibitor concentration. The obtained results were used to follow the Langmuir adsorption isotherm. Langmuir adsorption isotherm shows a graph between C/θ vs. C as shown in Fig. 4, which shows a straight line with the reaggregation coefficient (R^2) close to 1.It checks whether the *A. catechu* extract corresponds to the Langmuir adsorption isotherm and forms a monolayer on the surface of mild steel. That can be described as [26] follows:

$$\frac{C}{\theta} = \frac{1}{K_{\mathrm{ads}}} + C \tag{4}$$

$$\theta = \frac{\mathrm{IE}(\%)}{100} \tag{5}$$

where θ represents the surface coverage, inhibition concentration is represented by C, and K_{ads} represents the equilibrium adsorption constant. In the previous study, *M. fragrans* showed an effect of 83.27% inhibitory effect at 500 mg/L with K_{ads}(9.95 Lg^{-1}) whereas *A. catechu* showed a 91.13% inhibitory effect at 600 mg/L with K_{ads} (19.14 Lg^{-1}) and confirmed its better performance in the same corrosive medium.

Table 2 Corrosive properties of mild steel in 0.5 M H_2SO_4 without and at different concentrations of *A. catechu* for 24 h at 298 K

Inhibitor concentration (mg/L)	C_R (mmy^{-1})	Efficiency (IE%)	θ
00	11.33 ± 0.12	–	–
100	3.62 ± 0.12	68.06	0.6806
200	2.89 ± 0.12	74.41	0.7441
300	2.25 ± 0.13	80.10	0.8010
400	1.57 ± 0.12	86.12	0.8612
500	1.26 ± 0.11	88.79	0.8879
600	1.00 ± 0.13	91.13	0.9113

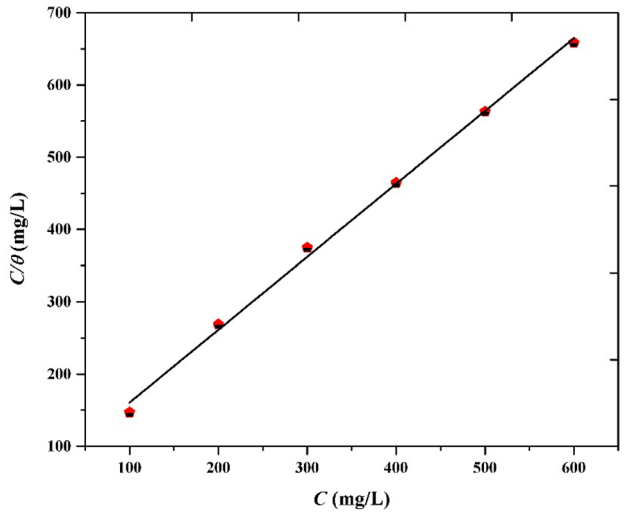

Fig. 4 The Langmuir adsorption isotherm (C/θ vs. C) by measuring the weight loss of the extract *A. catechu* for mild steel surface in 0.5 M H_2SO_4 at a temperature of 298 K for 24 h

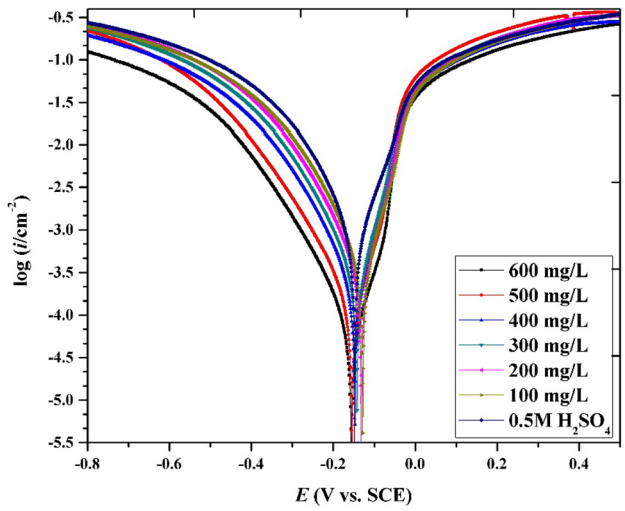

Fig. 5 Polarization curves of *A. catechu*on mild steel in 0.5 M H_2SO_4 for a concentration range of 0–600 mg/L extract at 298 K

3.3 Potentiodynamic Polarization Technique (Tafel)

Potentiodynamic polarization curves were recorded for mild steel in 0.5 M sulphuric acid solution absence and presence of various concentrations of *A. catechu* extract. Figure 5 shows the Tafel curves without and with the various concentration of *A. catechu* inhibitor in 0.5 M sulphuric acid. From the Tafel plots, we got the values for corrosion potential (E_{corr}), corrosion current density (i_{corr}), anodic and cathodic Tafel slopes ($\beta_a$andβ_c), and inhibition efficiency (IE %) using the following equitation [27]:

$$\mathrm{IE}(\%) = \frac{i^0_{corr} - i^i_{corr}}{i^0_{corr}} \times 100 \quad (6)$$

where i^0_{corr} and i^i_{corr} represent the corrosion current density in the absence of inhibitor and in the presence of inhibitor, respectively.

Table 3 shows the polarization parameters for the mild steel in the absence and presence of different concentrations of inhibitors. According to the table, the greater variability of the slopes of the anode table indicates its anodic response. The corrosive potential (E_{corr}) is within 85 mV in relation to the blank, suggesting its behaviour as a type of mixed inhibitor [28]. The Tafel curves show the fall in the value of the slopes of anodes and cathode curves with the addition of an inhibitor. This is due to the effect of the coating of active inhibitory molecules on the surface of the mild steel and the reduction of the solubility of the metal. At each addition of the concentration of the inhibitor, the density of the corrosion current (i_{corr}) continually decreases [29]. In the previous study, *M. fragrans* showed an effect of 87.42% inhibitory effect at 500 mg/L with i_{corr} (112.00 µA cm^{-2}) whereas *A. catechu* showed a 93.85% inhibitory effect at 600 mg/L with i_{corr}(54.70 µA cm^{-2}) and confirmed its better performance towards the same corrosive medium.

Table 3 Polarization parameters for mild steel in 0.5 M H_2SO_4 without and with different concentrations of *A. catechu* at 298 K

Inhibitor concentration (mg/L)	$-E_{corr}$ (mV vs. SCE)	i_{corr} (µA cm^{-2})	β_a (mV/dec)	$-\beta_c$ (mV/dec)	Efficiency (IE%)	θ
0	465	890.90	141.66	164.25	–	–
100	428	291.30	49.14	109.36	67.30	0.6730
200	432	251.30	47.98	110.38	71.79	0.7179
300	443	217.70	46.03	111.56	75.56	0.7556
400	447	157.80	44.36	110.81	82.28	0.8228
500	453	78.80	33.89	118.27	91.14	0.9114
600	483	54.70	33.30	101.95	93.85	0.9385

3.4 Electrochemical Impedance Spectroscopy (EIS)

To study the effect of *A. catechu* extract concentration, electrochemical impedance spectroscopy for mild steel was performed in 0.5 M sulphuric acid at 298 K to obtain a stable state. Figure 6a shows the equivalent circuit used to adapt to the results obtained. E_{OCP} (open circuit potential) was found relatively stable after 60 min of immersion, which indicates a stable condition. A constant phase element (CPE), a solution resistance (R_s), and a charge transfer resistance (R_{ct}) are the parts of the circuit. Using the following equations, it is better to explain the impedance of a constant phase element [30]:

$$Y_{CPE} = Y_0(j\omega)^n \tag{7}$$

$$Z_{CPE} = \left(\frac{1}{Y_0}\right)\left[(j\omega)_n\right]^{-1} \tag{8}$$

where Y_0 represents the proportional factor, and n explains the phase-shifting behaviour at different concentration. For $n = 0$, 0.5,1 and − 1, CPE represents to a resistance, Warburg component, capacitance, and inductance, respectively. The estimations of the double-layer capacitance (C_{dl}) can be acquired from the condition [31]:

$$C_{dl} = Y_0\left(\omega''_m\right)^{n-1} \tag{9}$$

where ω''_m represents the frequency of the impedance. The results are exhibited in Table 4. Figure 6b, c shows the Nyquist and Bode plots for mild steel in the absence and presence of the different concentration of *A. catechu* extract. The inhibition viability in connection to impedance was acquired by using the accompanying recipe [32]:

$$IE(\%) = \frac{R_{ct} - R^o_{ct}}{R_{ct}} \times 100 \tag{10}$$

where R_{ct} denotes the charge transfer resistance in the presence of the inhibitor and R^0_{ct} denotes the charge transfer resistance in the absence of the inhibitor.

As the concentration of inhibitors rises, the C_{dl} decreases and the R_{ct} rises as shown in Table 4. This can be attributed to a decrease in local dielectric constant and/or to enhance in the thickness of C_{dl}. The dissolution mechanism can be estimated from the value of the phase shift (n). The only constant on the Bode and Nyquist plots emphasized the load protection mechanism for coated and unprotected samples. Based on the Nyquist curves, in all cases, the highest performance was achieved at maximum concentration. It means with increase in the inhibitor concentration, the protective coating is formed.

Next, the results are plotted, showing a slight change in the value of n at different concentrations of inhibitors. Uniform n values reveal that the dissolution mechanism is controlled by the charge transfer process, both in the absence and in the presence of different concentrations of inhibitors [33, 34]. In the previous study, *M. fragrans* showed an effect of 87.88% inhibitory effect at 500 mg/L with R_{ct} (128.88 Ω cm^2) whereas *A. catechu* showed a 93.12% inhibitory effect at 600 mg/L with R_{ct}(228.56 Ω cm^2) and confirmed its better performance towards the same corrosive medium.

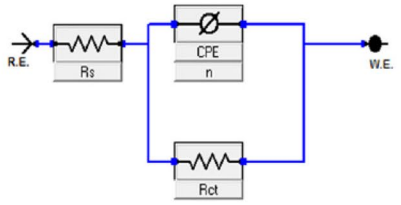

(a)

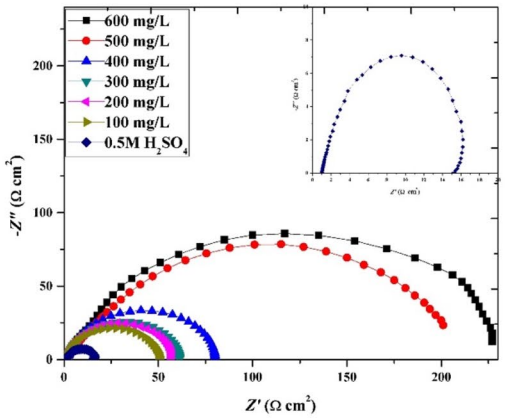

(b)

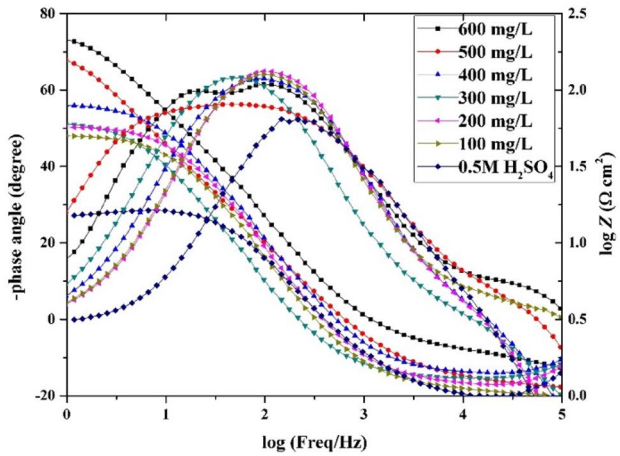

(c)

Fig. 6 **a** An equivalent circuit, **b** Nyquist and Bode c plots of mild steel in 0.5 M H_2SO_4 solution in the absence and presence of *A. catechu* extract

Table 4 EIS parameters of mild steel in 0.5 M H_2SO_4 without and at different concentrations of *A. catechu* at 298 K

Concentration of inhibitor (mg/L)	R_{ct} (Ω cm^2)	R_s (Ω cm^2)	f_{max} (Hz)	C_{dl} (μF cm^{-2})	n	Efficiency (IE%)	θ
0	15.71	1.22	37.60	269.00	0.57	–	–
100	49.74	0.98	9.77	228.00	0.70	68.42	0.6842
200	56.94	1.36	11.90	219.00	0.73	72.41	0.7241
300	61.07	1.51	4.54	176.00	0.76	74.27	0.7427
400	80.50	1.58	8.07	161.00	0.83	80.48	0.8048
500	215.20	1.13	5.49	140.00	0.88	92.70	0.9207
600	228.56	1.52	2.55	127.00	0.96	93.12	0.9312

3.5 SEM and AFM Analysis

Figure 7 highlights scanning electron microscopy (SEM) and atomic force microscopy (AFM) micrographs of mild steel surface prior and afterwards the corrosion tests without and with the inhibitor. Figure 7a shows the SEM and AFM micrographs of the abraded mild steel surface. It shows a sleek surface with least surface roughness (2.99 nm) and maximum height (60 nm) values. Figure 7b shows the mild steel surface after the corrosion test without the inhibitor. In this case, the mild steel surface is highly corroded due to the acidic corrosive media, resulting a rough micrograph with highest surface roughness (138.81 nm) and maximum height (2100 nm) values. Figure 7c shows the mild steel surface after the corrosion test with the inhibitor. It shows the presence of the inhibitor covers the surface and prevents the corrosion process with much lower surface roughness (26.46 nm) and maximum height (200 nm) values. It is very less than the outcomes obtained in the case of without inhibitor. It shows *A. catechu* is adsorbed on the surface of the mild steel creating a protective layer to prevent the corrosion process on the mild steel surface [35–37].

3.6 Theoretical Study Explanation

3.6.1 Quantum Chemical Calculations

Plant extracts have lots of phytochemical components. There are two main components of *A. catechu* selected for the theoretical study. *A. catechu* contains compound **[1]** and compound **[2]** as the main phytochemical components. Figure 8 shows the optimized, HOMO, and LUMO orbitals of the compound **[1]** and compound **[2]**. Following equations have been used to calculate different quantum chemical parameters:

$$\Delta E = E_{\mathrm{LUMO}} - E_{\mathrm{HOMO}} \tag{11}$$

$$\eta = \frac{1}{2}\left(E_{\mathrm{LUMO}} - E_{\mathrm{HOMO}}\right) \tag{12}$$

$$\chi = -\frac{1}{2}\left(E_{\mathrm{LUMO}} + E_{\mathrm{HOMO}}\right) \tag{13}$$

$$\Delta N = \frac{\chi_{\mathrm{Fe}} - \chi_{\mathrm{inh}}}{2\left(\eta_{\mathrm{Fe}} - \eta_{\mathrm{inh}}\right)} \tag{14}$$

$$\sigma = \frac{1}{\eta} \tag{15}$$

$$\Delta E_{\mathrm{BackDonation}} = -\frac{\eta}{4} \tag{16}$$

$$\pi = -\chi \tag{17}$$

where χ_{inh} and η_{inh} represent the electronegativity and hardness of inhibitor molecule, whereas χ_{inh} and η_{Fe} represent the electronegativity and hardness of iron, respectively. According to the Pearson's electronegativity scale, a value of 7 eV/mol has been taken for χ_{Fe}, and at the same time, 0 eV/mol has been taken for η_{Fe}.

Table 5 contains the basic properties of compound **[1]** and compound **[2]**, which are of great importance due to their effect on the interaction of electrons between the inhibitor molecule and the mild steel surface. We can see the values in Table 5, and compound **[2]** (− 1.46 eV) shows a high value of E_{HOMO} indicating its high capacity to deliver the charge to the mild steel. Compound **[2]** has the lowest values of E_{LUMO} (− 1.25 eV), which shows the highest capacity to receive electrons from Fe. Again compound **[2]** (0.21 eV) shows a high value of ΔE indicating its strong influence of the [Fe- compound **[2]**] complex. However, since these molecules change extensively for their concoction structures and any of them might exert a dominant impact under specific conditions and concentration, for example, if the examination states are fluctuate, specific characteristics might turn into upgrade alternately suppressed, which may prompt the change of the inhibition performance of *A. catechu* extract. As per the previous information, the phytochemical part secluded from the plant extricate showed moderately low extraction

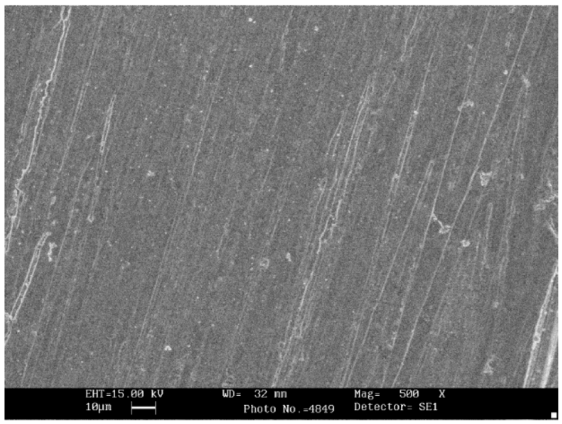

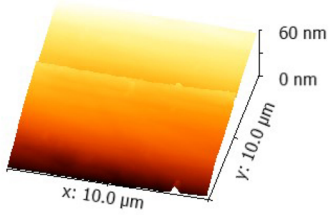

(a) Abrade mild steel

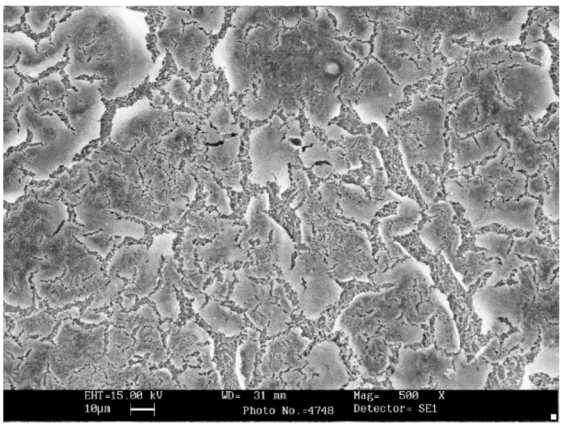

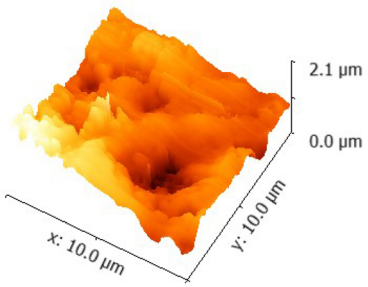

(b) Without inhibitor

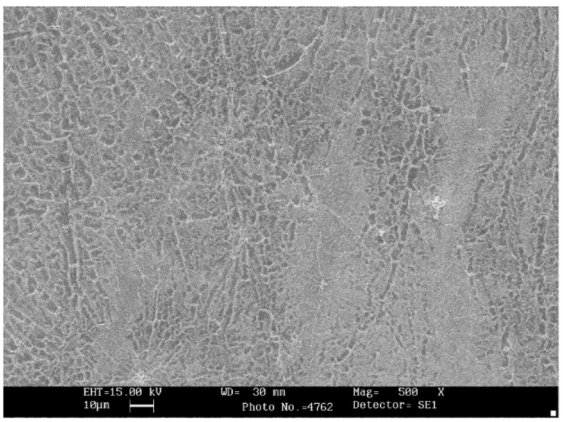

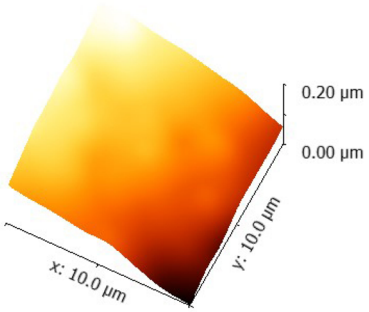

(c) With inhibitor

Fig. 7 AFM and SEM micrographs of the surface of mild steel after 24 h immersion at 298 K in 0.5 M H_2SO_4 **a** abrade soft steel, **b** without inhibitor and **c** with inhibitor

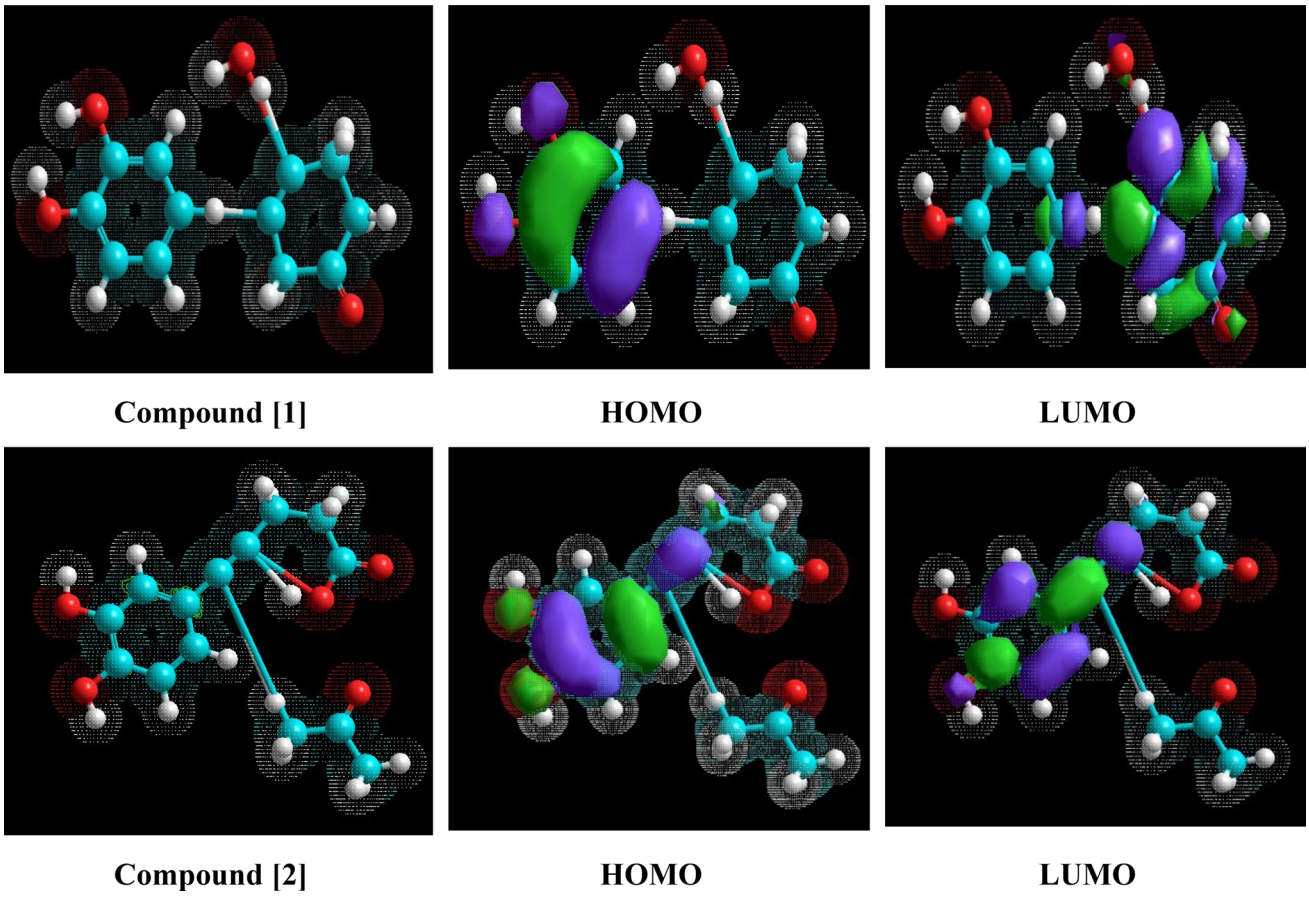

Fig. 8 Optimized structures and frontier molecular orbital density distributions (HOMO & LUMO) of Compound **[1]** and Compound **[2]** obtained by DFT/B3LYP/6-31G+(d,p) method

Table 5 Quantum chemical parameters calculated for the Compound **[1]** and Compound **[2]** molecules by the method DFT/B3LYP/6-31G+(d, p)

Molecule	E_{HOMO}(eV)	E_{LUMO}(eV)	ΔE (eV)	ΔN (e)	$\Delta E_{Back\text{-}Donation}$ (eV)	η (eV)	σ (eV^{-1})	χ (eV)	π (eV)
Compound **[1]**	−3.91	−1.24	2.67	1.65	−0.33	1.33	0.74	2.50	−2.50
Compound **[2]**	−2.04	−1.58	0.45	11.37	−0.05	0.22	4.38	1.81	−1.81

productivity contrasted with a mix of various phytochemical substances, which means a mix of compound **[1]** and compound **[2]** delivers preferred outcomes over independent [38, 39].

3.7 A Proposed Mechanism of Action

To explain the inhibitory effect of *A. catechu* on mild steel in 0.5 M H_2SO_4, it is important to evaluate the experimental and calculated results and correlate them with the structural, chemical and electronic properties of the inhibitory molecules. *A. catechu* contains several phytochemical compounds that take into account the number of heteroatoms and aromatic rings. These compounds act as Lewis bases and form coordination bonds with the free *d*-orbital of Fe and adsorb on a mild steel surface to form a protective layer on the mild steel surface to protect against corrosive environments. The HOMO orbitals of the molecules studied indicate that a uniform pair of electrons is available for nucleophilic interaction (chemisorption) with the mild steel surface. The LUMO in the heteroatoms causes the formation of dπ–dπ bonds, and the formation of superimposed three-dimensional electrons of iron atoms with a free spatial orbital heteroatom is possible. Also, the adsorption can be done by electrostatic interaction (physisorption) between heteroatoms and the Fe^{2+}. Retrospection can be done using π-electrons of aromatic rings. This phenomenon is also verified by theoretical studies and polarization measurements. Figure 9 shows the proposed mechanism for the phenomenon of compound **[2]** molecule adsorption on a mild steel surface [40–43].

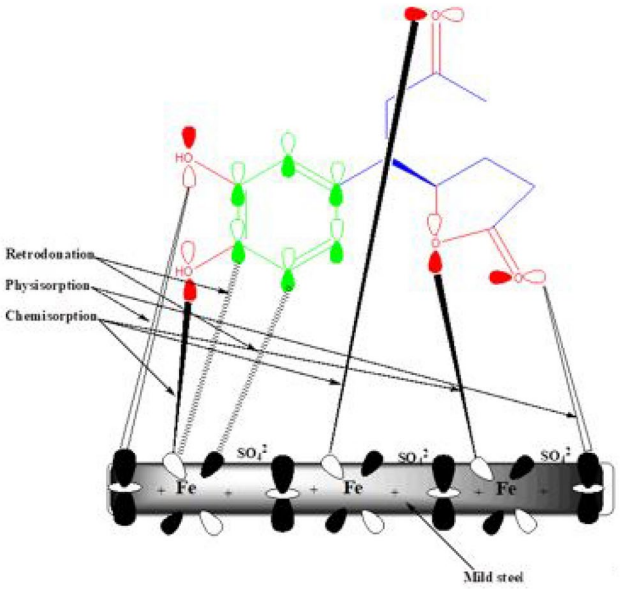

Fig. 9 Suggested mechanism of adsorption behaviour of the Compound **[2]** molecule on a mild steel surface

4 Conclusion

The corrosion control effect of *A. catechu* in a corrosive environment of 0.5 M sulphuric acid for mild steel has been tested by electrochemical analysis followed by weight loss test, UV–vis., FT-IR, AFM, SEM and computational studies. The conclusions of this assessment are as follows:

I. Electrochemical tests and weight loss confirmed that *A. catechu* indicates > 91% of corrosion prevention efficiency at 600 mg/L.
II. The presence of several active functional groups found in *A. catechu* has been confirmed by FT-IR and the adsorption phenomenon has been confirmed by UV–vis. spectroscopy technique.
III. The most important phytochemicals of the extract were simulated with DFT, and the results confirm the experimental results.
IV. SEM supported by AFM confirmed the surface adsorption of *A. catechu* on the mild steel surface.

Acknowledgements We are very thankful to Prof. Gurmeet Singh, Department of Chemistry, University of Delhi, Delhi (INDIA), for providing the lab facility for electrochemical experiments.

Compliance with Ethical Standards

Conflict of interest Authors declare there is no conflict of interest.

References

1. Ahamad I, Prasad R, Quraishi MA (2010) Experimental and quantum chemical characterization of the adsorption of some Schiff base compounds of phthaloyl thiocarbohydrazide on the mild steel in acid solutions. Mater Chem Phys 124:1155–1165
2. Abd El-Lateef HM, Abo-Riya MA, Tantawy AH (2016) Empirical and quantum chemical studies on the corrosion inhibition performance of some novel synthesized cationic gemini surfactants on carbon steel pipelines in acid pickling processes. Corros Sci 108:94–110
3. Shahabi S, Norouzi P, Ganjali MR (2015) Electrochemical and theoretical study of the inhibition effect of two synthesized thiosemicarbazide derivatives on carbon steel corrosion in hydrochloric acid solution. RSC Adv 5:20838–20847
4. Bagga MK, Gadi R, Yadav OS, Kumar R, Chopra R, Singh G (2016) Investigation of phytochemical components and corrosion inhibition property of *Ficus racemosa* stem extract on mild steel in H_2SO_4 medium. J Environ Chem Eng 4:4699–4707
5. Hassan KH, Khadom AA, Kurshed NH (2016) *Citrus aurantium* leaves extracts as a sustainable corrosion inhibitor of mild steel in sulfuric acid. S Afr J Chem Eng 22:1–5
6. Patel N, Rawat A, Jauhari S, Mehta G (2010) Inhibitive action on *Bridelia restusa* leaves extract on corrosion of mild steel in acidic media. Eur J Chem 1:129–133
7. Ibrahim T, Alayan H, Al Mowaqet Y (2012) The effect of Thyme leaves extract on corrosion of mild steel in HCl. Prog Org Coat 75:456–462
8. Al-Otaibi MS et al (2013) The effect of temperature on the corrosion inhibition of mild steel in 1 M HCL solution by *Curcuma longa* extract. Int J Electrochem Sci 5:847–859
9. Vasudha VG, Shanmuga Priya K (2013) *Polyalthia longifolia* as a corrosion inhibitor for mild steel in HCl solution. Res J Chem Sci 3:21–26
10. Garai S, Garai S, Jaisankar P, Singh JK, Elango A (2012) A comprehensive study on crude methanolic extract of *Artemisia pallens* (Asteraceae) and its active component as effective corrosion inhibitors of mild steel in acid solution. Corros Sci 60:193–204
11. Rose K, Kim BS, Rajagopal K, Arumugam S, Devarayan K (2016) Surface protection of steel in acid medium by *Tabernaemontana divaricata* extract: physicochemical evidence for adsorption of inhibitor. J Mol Liq 214:111–116
12. Oguzie EE, Chidiebere MA, Oguzie KL, Adindu CB, Momoh-Yahaya H (2014) BioLC-MS extracts for materials protection: corrosion inhibition of mild steel in acidic media by *Terminalia chebula* extracts. Chem Eng Commun 201:790–803
13. Soltani N, Tavakkoli N, Khayatkashani M, Jalali MR, Mosavizade A (2012) Green approach to corrosion inhibition of 304 stainless steel in hydrochloric acid solution by the extract of *Salvia officinalis* leaves. Corros Sci 62:122–135
14. Ji G, Anjum S, Sundaram S, Prakash R (2015) *Musa paradisica* peel extract as green corrosion inhibitor for mild steel in HCl solution. Corros Sci 90:107–117
15. Pal S, Lgaz H, Tiwari P, Chung IM, Ji G, Prakash R (2019) Experimental and theoretical investigation of aqueous and methanolic extracts of *Prunus dulcis* peel as green corrosion inhibitors of mild steel in aggressive chloride media. J Mol Liq 276:347–361
16. Tammam RH, Fekry AM, Saleh MM (2016) Understanding different inhibition actions of surfactants for mild steel corrosion in acid solution. Int J Electrochem Sci 11:1310–1326
17. Ameer MA, Fekry AM (2015) Corrosion inhibition by naturally occurring *Hibiscus sabdariffa* plant extract on mild steel alloy in HCl solution. Tur J Chem 39:1078–1088
18. Ahmed RA, Farghali RA, Fekry AM (2012) Study for the stability and corrosion inhibition of electrophoretic deposited chitosan

on mild steel alloy in acidic medium. Int J Electrochem Sci 7:7270–7282
19. Fekry AM, Ameer MA (2011) Electrochemical investigation on the corrosion and hydrogen evolution rate of mild steel in sulphuric acid solution. Int J Hydrogen Energy 36:11207–11215
20. Ameer MA, Fekry AM (2011) Corrosion inhibition of mild steel by natural product compound. Prog Org Coat 71:343–349
21. Fekry AM, Gasser AA, Ameer MA (2010) Corrosion protection of mild steel by polyvinylsilsesquioxanes coatings in 3% NaCl solution. J Appl Electrochem 40:739–747
22. Singh K, Lal B (2006) Notes on traditional uses of khair (*Acacia catechu* Willd.) by inhabitants of Shivalik range in Western Himalaya. Ethnobot Leafl 10:109–112
23. Li XC, Yang LX, Wang HQ, Chen RY (2011) Phenolic compounds from the aqueous extract of *Acacia catechu*. Chinese Chem Lett 22:1331–1334
24. Haldhar R, Prasad D, Saxena A, Singh P (2018) *Valeriana wallichi* root extract as a green & sustainable corrosion inhibitor for mild steel in acidic environments: experimental and theoretical study. Mater Chem Front 2:1225–1237
25. Haldhar R, Prasad D, Saxena A (2018) *Myristica fragrans* extract as an eco-friendly corrosion inhibitor for mild steel in 0.5 M H_2SO_4. J Environ Chem Eng 6:2290–2301
26. Saxena A, Prasad D, Haldhar R (2018) Investigation of corrosion inhibition effect and adsorption activities of *Cuscuta reflexa* extract for mild steel in 0.5 M H_2SO_4. Bioelechemistry. https://doi.org/10.1016/j.bioelechem.2018.07.006
27. Saxena A, Prasad D, Haldhar R (2018) Investigation of corrosion inhibition effect and adsorption activities of *Achyranthes aspera* extract for mild steel in 0.5 M H_2SO_4. J Fail Anal Prev. https://doi.org/10.1007/s11668-018-0491-8
28. Bhardwaj N, Prasad D, Haldhar R (2018) Study of the Aegle marmelos as a green corrosion inhibitor for mild steel in acidic medium: experimenta and theoretical approach. J Bio Tribo-Corros 4:1–10
29. Salarvand Z, Amirnasr M, Talebian M, Raeissi K, Meghdadi S (2017) Enhanced corrosion resistance of mild steel in 1M HCl solution by trace amount of 2-phenyl-benzothiazole derivatives: experimental, quantum chemical calculations and molecular dynamics (MD) simulation studies. Corros Sci 114:133–145
30. Saxena A, Prasad D, Haldhar R (2018) Use of *Asparagus racemosus* extract as green corrosion inhibitor for mild steel in 0.5 M H_2SO_4. J Mater Sci 53:8523–8535
31. Deng S, Li X (2012) Inhibition by Ginkgo leaves extract of the corrosion of steel in HCl and H_2SO_4 solutions. Corros Sci 55:407–415
32. Kumar R, Yadav OS, Singh G (2017) Electrochemical and surface characterization of a new eco-friendly corrosion inhibitor for mild steel in acidic media: a cumulative study. J Mol Liq 237:413–427
33. Morad MS (2000) An electrochemical study on the inhibiting action of some organic phosphonium compounds on the corrosion of mild steel in aerated acid solutions. Corros Sci 42:1307–1326
34. Fekry AM, Shehata M, Azab SM, Walcarius A (2020) Voltammetric detection of caffeine in pharmacological and beverages samples based on simple nano- Co (II, III) oxide modified carbon paste electrode in aqueous and micellar media. Sens Actuators B 302:127–172
35. Haldhar R, Prasad D, Saxena A, Kumar A (2018) Experimental and theoretical studies of *Ficus religiosa* as green corrosion inhibitor for mild steel in 0.5 M H_2SO_4 solution. Sustain Chem Pharm 9:95–105
36. Haldhar R, Prasad D, Saxena A (2018) *Armoracia rusticana* as sustainable and eco-friendly corrosion inhibitor for mild steel in 0.5 M sulphuric acid: experimental and theoretical investigations. J Environ Chem Eng 6:5230–5238
37. Verma C, Quraishi MA, Ebenso EE, Obot IB, El Assyry A (2016) 3-Amino alkylated indoles as corrosion inhibitors for mild steel in 1M HCl: experimental and theoretical studies. J Mol Liq 219:647–660
38. El-TaibHeakal F, Fekry AM (2009) Experimental and theoretical study of Uracil and Adenine inhibitors in Sn-Ag alloy/nitric acid corroding system. J Electrochem Soc 155:C534–542
39. Haldhar R, Prasad D, Saxena A, Kaur A (2018) Corrosion resistance of mild steel in 0.5 M H_2SO_4 solution by plant extract of *Alkana tinctoria*: experimental and theoretical studies. Eur Phys J Plus 133:356
40. Fekry AM, Ghoneim AA, Ameer MA (2014) Electrochemical impedance spectroscopy of chitosan coated magnesium alloys in a synthetic sweat medium. Surf Coat Technol 283:126–132
41. Ahmed RA, Fekry AM (2013) Preparation and characterization of a nanoparticles modified chitosan sensor and its application for the determination of heavy metals from different aqueous media. Int J Electrochem Sci 8:6692–6708
42. El-TaibHeakal F, Fekry AM, Fatayerji MZ (2009) Electrochemical behavior of AZ91D magnesium alloy in phosphate medium—part II. Induced passivation. J Appl Electrochem 39:1633–1642
43. El-TaibHeakal F, Fekry AM, Fatayerji MZ (2009) Electrochemical behavior of AZ91D magnesium alloy in phosphate medium—part I. Effect of pH. J Appl Electrochem 39:583–591